

# High-Resolution Spectroscopic Study of the (310) Local Mode Combination Band System of AsH<sub>3</sub>

Hai Lin, Oleg N. Ulenikov,<sup>1</sup> Sergi Yurchinko,<sup>1</sup> Xiao-gang Wang, and Qing-shi Zhu<sup>2</sup>

*Department of Chemical Physics, University of Science and Technology of China, Hefei 230026, People's Republic of China*

Received July 31, 1997; in revised form September 26, 1997

The high-resolution spectra of AsH<sub>3</sub> in the 8130–8340 cm<sup>-1</sup> region, which were assigned to the (310; A<sub>1</sub>), and (310; E<sub>1</sub>), and the (310; E<sub>2</sub>) local mode combination bands, have been recorded at a resolution of 0.01 cm<sup>-1</sup> and rotationally analyzed. The spectroscopic parameters were obtained by least-squares fitting. The rotational energy levels were fitted for the (310; A<sub>1</sub>) state (21 levels in all) up to  $J = 5$ , for the (310; E<sub>2</sub>) state (43 levels in all) up to  $J = 7$ , and for the (310; E<sub>1</sub>) state (43 levels in all) up to  $J = 5$ . The complication of the rotational structure indicates rotational perturbation. © 1998 Academic Press

## 1. INTRODUCTION

The rotational energy level structure of the vibrational–rotational spectra of small symmetric molecules has been the subject of great interest in recent years due to its unusual features near the local mode limit. As good examples for the exploration of local mode behavior of symmetric top molecules, the pyramid-type molecules XH<sub>3</sub> ( $X = \text{N, P, As, Sb}$ ) have been extensively studied. Coy and Lehmann studied the five- and six-quanta overtone of NH<sub>3</sub> ( $I$ ). The spectra were found to be complicated owing to the coupling between stretching and bending vibrational modes. Fermi resonance is also discussed for PH<sub>3</sub> ( $2$ ). However, AsH<sub>3</sub> and SbH<sub>3</sub> are the better molecules to study not only because they are closer to the local mode limit but also because their bending fundamentals are significantly lower than half of the stretching modes. Vibrational analysis was carried out for AsH<sub>3</sub> and SbH<sub>3</sub> with a simple local mode model ( $3$ ). Rotational analysis has been performed for the SbH<sub>3</sub> (200) ( $4$ ), (300) ( $5$ ), and (400) ( $6$ ) bands and for the AsH<sub>3</sub> (200) ( $7$ ), (300) ( $8$ ), and (400) ( $9$ ) bands. The striking phenomenon of rotational requantization and symmetry reduction at the local mode limit was demonstrated clearly in the AsH<sub>3</sub> (400) bands ( $9$ ). However, the vibrational–rotational spectra of the (600) band of AsH<sub>3</sub> were found to be perturbed ( $10$ ).

Recently, high-resolution spectra from 5900 to 11 500 cm<sup>-1</sup> of AsH<sub>3</sub> have been recorded and rotationally analyzed in our laboratory. Here we present a detailed rotational analysis of the (310) local mode combination band of AsH<sub>3</sub>.

<sup>1</sup> Laboratory of Molecular Spectroscopy, Physics Department, Tomsk State University, Tomsk 634050, Russia.

<sup>2</sup> To whom correspondence should be addressed.

## 2. EXPERIMENTAL ARRANGEMENT

AsH<sub>3</sub> with a stated purity of 99.99% was purchased from the Nanjing Special Gas Company. The high-resolution spectrum was recorded at room temperature on a Bruker IFS 120 HR Fourier transform spectrometer, which was equipped with a CaF<sub>2</sub> beamsplitter, an InSb detector, and a tungsten halogen source. A White-type multipass cell with a 105-m effective path length was used. Because of the wide range of the spectra to be measured, no optical filter was used but electronic filters were employed. The sample pressure was 13 Torr. The unapodized resolution is 0.01 cm<sup>-1</sup>. (The estimated Doppler width of AsH<sub>3</sub> at room temperature is 0.01 cm<sup>-1</sup> near 8000 cm<sup>-1</sup>.) Ninety separate spectra were obtained, each resulting from 25 coadded scans. Then the 90 spectra, which amount to 2250 scans in all, were averaged point by point to improve the SNR. The accuracy of the line position was estimated as 0.005 cm<sup>-1</sup>.

The band from 8130 to 8340 cm<sup>-1</sup> was assigned to the (310) combination band, which consists of the (310; A<sub>1</sub>) band, the (310; E<sub>2</sub>) band, and the (310; E<sub>1</sub>) band, according to local mode vibrational analysis ( $3$ ). Here the (310; E<sub>2</sub>) label denotes the  $E$  band, the band center of which is high, while the (310; E<sub>1</sub>) label denotes the other  $E$  bands, the band center of which is low. Parts of the spectrum of the (310; A<sub>1</sub>), (310; E<sub>1</sub>), and (310; E<sub>2</sub>) bands are illustrated in Fig. 1. The label  $\Gamma_v: J''K''\Gamma_r'' \leftarrow \Gamma_v: J'K'\Gamma_r'$  denotes the transition from the ground level to the upper level, where  $\Gamma_v$  is the vibrational symmetry and  $\Gamma_r$  is the vibrational–rotational symmetry.

The calibration was carried out by comparing the residual H<sub>2</sub>O lines with the data of Ref. ( $11$ ).

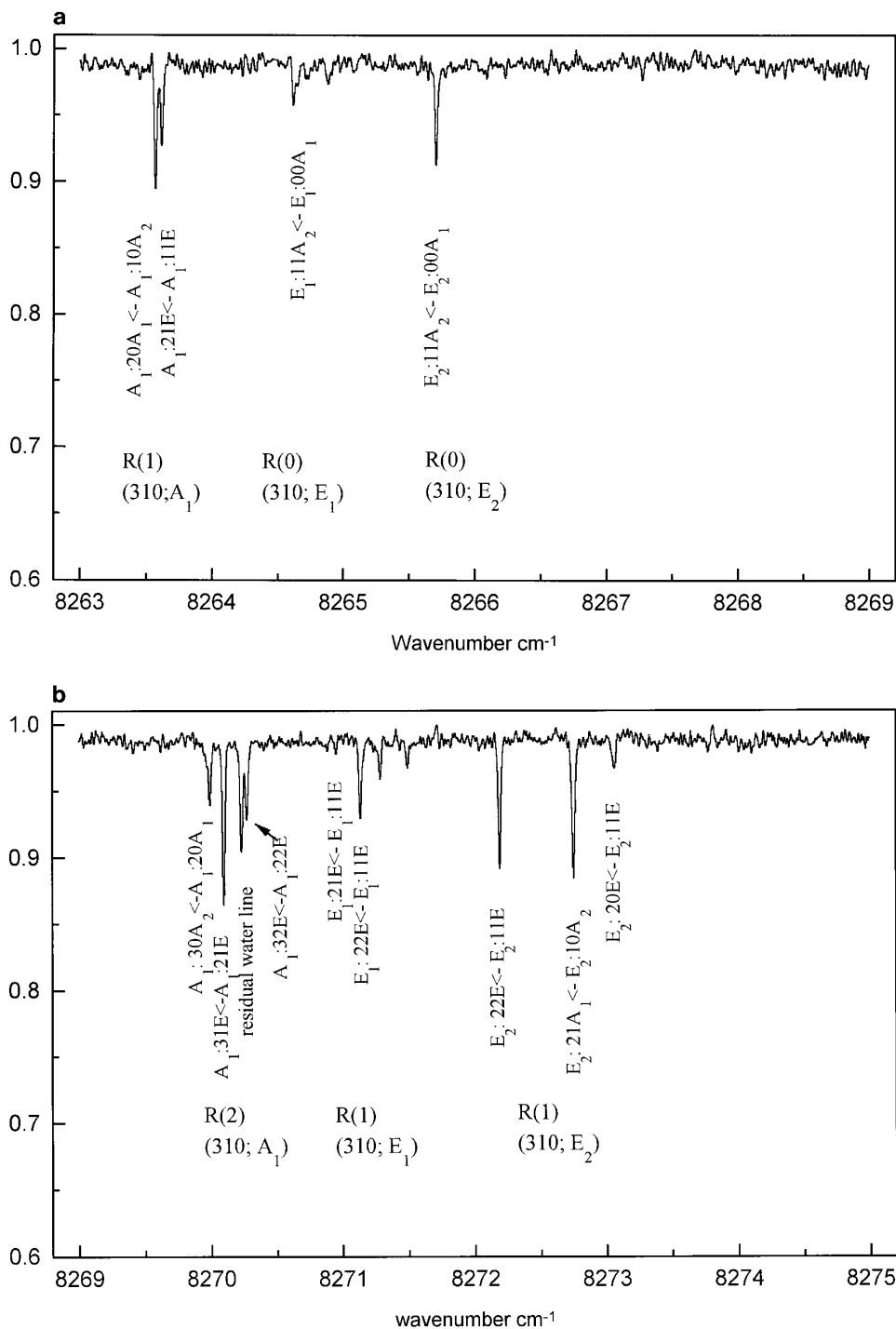


**FIG. 1.** Parts of the spectrum of the  $(310; A_1)$ ,  $(310; E_1)$ , and  $(310; E_2)$  bands. The label  $\Gamma_v:J'K'\Gamma_r' - \Gamma_v:J''K''\Gamma_r''$  denotes the transition from the ground level (double primed) to the upper level (single primed), where  $\Gamma_v$  is the vibrational symmetry and  $\Gamma_r$  is the vibrational-rotational symmetry. It can be seen that the  $(310; A_1)$  band and the  $(310; E_2)$  band are strong in intensity while the  $(310; E_1)$  band is weak. (a)  $R(1)$  of the  $(310; A_1)$  region; (b)  $R(2)$  of the  $(310; A_1)$  region; (c)  $R(3)$  of the  $(310; A_1)$  region; (d)  $R(4)$  of the  $(310; A_1)$  region. It can be seen that the vibrational-rotational bands of  $(310; E_1)$  and  $(310; E_2)$  are shifted to higher energy, so that the  $R(J)$  of  $(310; E_1)$  and  $(310; E_2)$  are located in same region of  $R(J + 1)$  of  $(310; A_1)$ .

### 3. VIBRATIONAL-ROTATIONAL ASSIGNMENT

It can be seen from Fig. 1 that the  $(310; A_1)$  band and the  $(310; E_2)$  band are strong in intensity while the  $(310; E_1)$

band is weak. The transitions were assigned by the ground state combination difference method (GSCD). The energy levels of the ground state are obtained from Ref. (12). The spectroscopic parameters were obtained by least-squares fit-

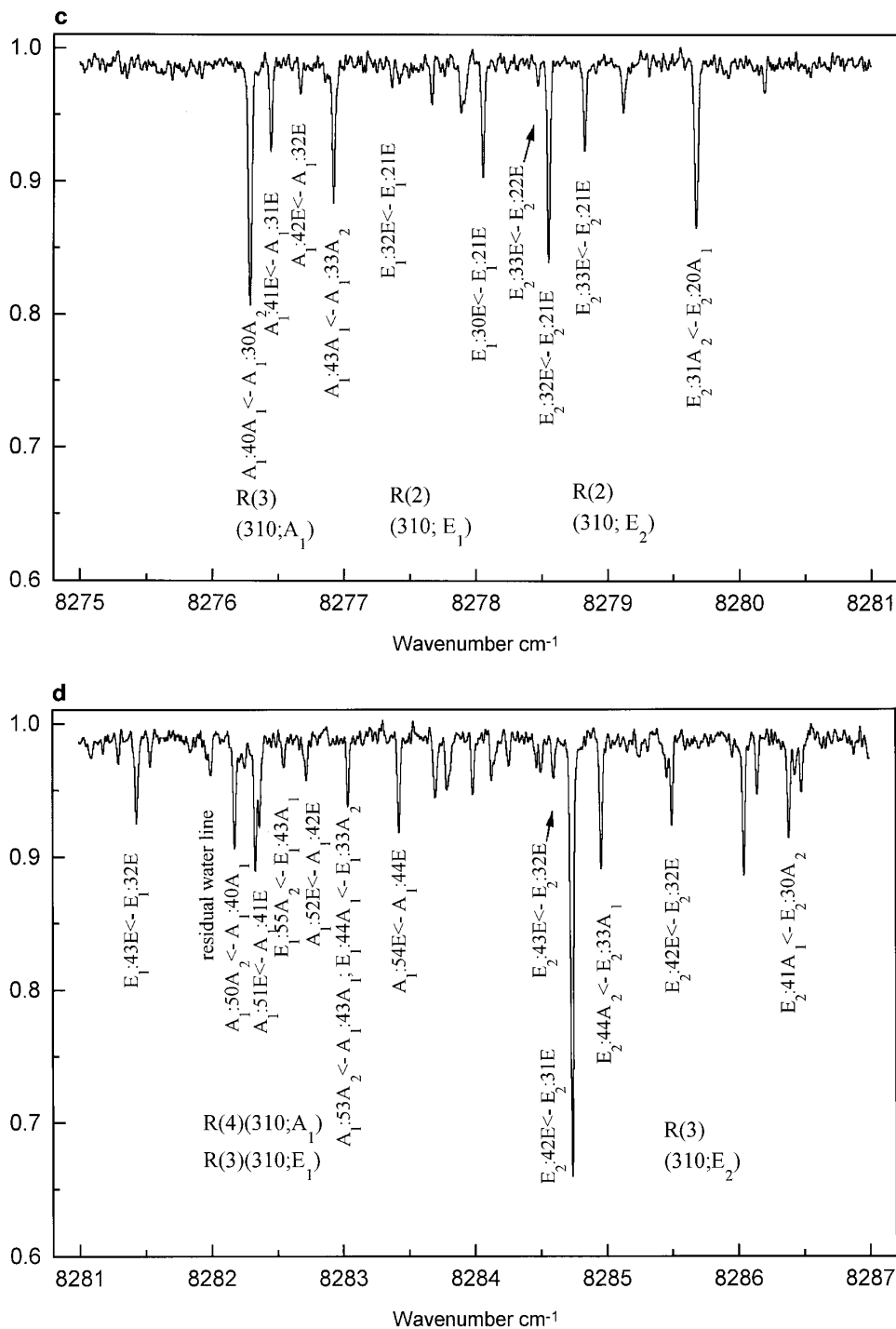


FIG. 1—Continued

ting, and the upper state energy levels were obtained from the assigned lines (Tables 2 and 3).

The spectrum is complicated due to perturbation and the  $K$  structure is destroyed when  $J > 4$  for the (310;  $A_1$ ) band. Lines found by combination differences are too far away in frequency. The  $K$  structure of the (310;  $E_1$ ) and (310;  $E_2$ ) bands cannot be observed at all. For the (310;  $A_1$ ) band,

45 transitions were assigned. Combination differences with three allowed transitions (from the  $P$ ,  $Q$ , and  $R$  branches) can be found with certainty for most of the upper level of the (310;  $A_1$ ) band. A few transitions of  $\Delta k = 3$  were also found. However, it is much different in the case of the (310;  $E_2$ ) band, in which 94 transitions were assigned. The combination differences with three allowed transitions (from

**TABLE 1**  
**Fitting Spectroscopic Parameters of the (310) Band of AsH<sub>3</sub>**

	$\langle 310; A_1   310; A_1 \rangle$	$\langle 310; E_2   310; E_2 \rangle$	$\langle 310; E_1   310; E_1 \rangle$
$\nu_0 / \text{cm}^{-1}$	8249.521(20)	8258.384(14)	8257.2726(75)
$B / \text{cm}^{-1}$	3.5889(12)	3.65223(70)	3.58302(44)
$C / \text{cm}^{-1}$	3.4084(76)	3.4555(26)	3.32346(56)
$D_{Jk} / \text{cm}^{-1}$	-0.00154(45)		
$D_k / \text{cm}^{-1}$	0.00230(64)		
$C\zeta / \text{cm}^{-1}$		-0.1218(73)	-0.2394(40)
$\eta_J / \text{cm}^{-1}$		-0.03984(75)	0.00314(39)
$\eta_k / \text{cm}^{-1}$		-0.0223(21)	-0.0539(10)
$\eta_{Jk} / \text{cm}^{-1}$		0.002310(83)	0.001784(33)
$r_{\text{eff}} / \text{cm}^{-1}$		-0.00579(62)	
$q_{\text{eff}} / \text{cm}^{-1}$		0.0652(28)	-0.0288(30)
$q_{\text{eff}}^J / \text{cm}^{-1}$		0.000677(69)	0.00046(12)
	$\langle 310; A_1   310; E_2 \rangle$		
$\alpha_{\text{eff}}^{\text{zx}} / \text{cm}^{-1}$	-0.319(35)		
$\alpha_{\text{eff}}^{\text{zx}J} / \text{cm}^{-1}$	0.0090(20)		
rms	0.04		0.02

the  $P$ ,  $Q$ , and  $R$  branches) cannot be found for many of the upper levels; instead, only two allowed transitions (from the  $P$ ,  $Q$ , and  $R$  branches) are found. Forbidden transitions of  $\Delta k = 0, 2$ , and  $3$  are found at the same time. There were 72 transitions of the  $(310; E_1)$  band assigned, and in this case only a few combination differences with three allowed transitions could be found; instead, only one or two branches of three allowed transitions (from the  $P$ ,  $Q$ , and  $R$  branches) and/or forbidden transitions are found for most of the upper levels.

We first assigned the low  $J$  energy level with  $k = 0$  and  $k = 1$ , which was fitted to a simple Hamiltonian involving only  $\nu$ ,  $B$ , and  $C$  parameters. Then these parameters were used to predict additional upper energy levels which were compared with the observed levels. Then we assigned more lines, which are fitted to give rise to more higher order parameters. The steps were repeated until the transitions were assigned up to  $J = 5$  for the  $(310; A_1)$  band, and up to  $J = 7$  for both the  $(310; E_2)$  band and the  $(310; E_1)$  band. For some upper levels, because no combination difference can be found at all, we used the calculated value to assign the observed transitions. When  $J$  is higher than 4 for the  $(310; E_2)$  and the  $(310; E_1)$  states, it is difficult to assign the  $J$  and  $K$  quantum numbers for some upper energy levels due to the mixing of the wavefunctions.

It is interesting to find that the intensities of some forbidden transitions of the  $(310; E_1)$  band and a few forbidden

transitions of the  $(310; E_2)$  band are strong compared with the transitions normally allowed. When  $J$  is higher, it is difficult to determine the correct combination from many pairs of lines which satisfy the combination difference because of the high density of lines in the  $Q$  branch.

The spectroscopic parameters which were obtained by least-squares fitting are listed in Table 1. Table 2 lists the calculated and observed rotational energy levels for the  $(310; A_1)$  state (21 levels in all) up to  $J = 5$  and for the  $(310; E_2)$  state (43 levels in all) up to  $J = 7$ , and Table 3 lists the energy levels for the  $(310; E_1)$  state (43 levels in all) up to  $J = 5$ . The number of transitions used in the GSCD method for every energy level is given in the last column.

The standard deviation of the fit is  $0.04 \text{ cm}^{-1}$  for the  $(310; A_1)$  and  $(310; E_2)$  bands, and  $0.02 \text{ cm}^{-1}$  for the  $(310; E_1)$  band, which is satisfactory compared with the experimental uncertainty of  $0.01 \text{ cm}^{-1}$ . Some high-order parameters, e.g.,  $B\xi\Omega$ ,  $B\xi^{(J)}$ , and  $\alpha^{\text{xx}}$ , were constrained to zero in the fitting. Without further physical information, it is difficult to determine which parameters should be constrained.

#### 4. THE VIBRATIONAL-ROTATIONAL MATRIX ELEMENTS

In our fitting, we took the coupling between the rovibrational levels of the  $(310; A_1)$  band and the  $(310; E_2)$  band

**TABLE 2**  
**Energy Levels (cm<sup>-1</sup>) of the 310; A<sub>1</sub> State**  
**and the 310; E<sub>2</sub> State of AsH<sub>3</sub>**

J	K	Sym. of Vib.	Sym.	Obs.	Cal.	Obs.-Cal.	N <sup>a</sup>
0	0	A <sub>1</sub>	A <sub>1</sub>	8249.488	8249.521	-.033	1
0	0	E <sub>2</sub>	E	8258.366	8258.384	-.018	1
1	1	E <sub>2</sub>	A <sub>1</sub>	8265.613	8265.571	.042	1
1	0	A <sub>1</sub>	A <sub>2</sub>	8256.698	8256.694	.004	2
1	1	E <sub>2</sub>	A <sub>2</sub>	8265.710	8265.709	.001	1
1	1	A <sub>1</sub>	E	8256.500	8256.517	-.017	1
1	0	E <sub>2</sub>	E	8265.704	8265.691	.013	1
1	1	E <sub>2</sub>	E	8265.321	8265.344	-.023	1
2	0	A <sub>1</sub>	A <sub>1</sub>	8271.079	8271.043	.036	3
2	1	E <sub>2</sub>	A <sub>1</sub>	8280.259	8280.320	-.061	2
2	2	E <sub>2</sub>	A <sub>1</sub>	8279.539	8279.562	-.023	1
2	1	E <sub>2</sub>	A <sub>2</sub>	8279.977	8279.904	.073	2
2	2	E <sub>2</sub>	A <sub>2</sub>	8279.540	8279.554	-.014	1
2	1	A <sub>1</sub>	E	8270.874	8270.839	.035	3
2	2	A <sub>1</sub>	E	8270.273	8270.301	-.028	2
2	0	E <sub>2</sub>	E	8280.314	8280.335	-.021	3
2	1	E <sub>2</sub>	E	8280.101	8280.132	-.031	2
2	2	E <sub>2</sub>	E	8279.445	8279.460	-.015	2
3	3	A <sub>1</sub>	A <sub>1</sub>	8290.856	8290.869	-.013	2
3	1	E <sub>2</sub>	A <sub>1</sub>	8301.356	8301.334	.022	1
3	2	E <sub>2</sub>	A <sub>1</sub>	8301.958	8301.945	.013	1
3	0	A <sub>1</sub>	A <sub>2</sub>	8292.610	8292.575	.035	2
3	3	A <sub>1</sub>	A <sub>2</sub>	8290.856	8290.869	-.013	2
3	1	E <sub>2</sub>	A <sub>2</sub>	8302.187	8302.264	-.077	3
3	2	E <sub>2</sub>	A <sub>2</sub>	8301.958	8301.889	.069	1
3	1	A <sub>1</sub>	E	8292.358	8292.358	-.000	2
3	2	A <sub>1</sub>	E	8291.771	8291.750	.021	3
3	0	E <sub>2</sub>	E	8302.285	8302.274	.011	2
3	1	E <sub>2</sub>	E	8302.449	8302.358	.091	2
3	2	E <sub>2</sub>	E	8300.813	8300.834	-.021	3
3	3	E <sub>2</sub>	E	8301.090	8301.109	-.019	4
3	3	E <sub>2</sub>	E	8299.978	8299.970	.008	3
4	0	A <sub>1</sub>	A <sub>1</sub>	8321.298	8321.290	.008	3
4	3	A <sub>1</sub>	A <sub>1</sub>	8319.657	8319.572	.085	3
4	1	E <sub>2</sub>	A <sub>1</sub>	8331.400	8331.375	.025	2
4	2	E <sub>2</sub>	A <sub>1</sub>	8331.766	8331.730	.036	1
4	4	E <sub>2</sub>	A <sub>1</sub>	8327.699	8327.698	.001	3
4	1	E <sub>2</sub>	A <sub>2</sub>	8329.922	8329.948	-.026	2
4	1	A <sub>1</sub>	E	8321.047	8321.096	-.049	2
4	2	A <sub>1</sub>	E	8320.449	8320.518	-.069	3
4	4	A <sub>1</sub>	E	8318.245	8318.242	.003	2
4	0	E <sub>2</sub>	E	8331.714	8331.676	.038	1
4	1	E <sub>2</sub>	E	8331.831	8331.898	-.067	1
4	2	E <sub>2</sub>	E	8329.498	8329.493	.005	4
4	3	E <sub>2</sub>	E	8330.805	8330.774	.031	3
4	3	E <sub>2</sub>	E	8328.548	8328.544	.004	2
4	4	E <sub>2</sub>	E	8329.078	8329.082	-.004	3
5	1	E <sub>2</sub>	A <sub>1</sub>	8365.682	8365.712	-.030	2
5	0	A <sub>1</sub>	A <sub>2</sub>	8357.179	8357.188	-.009	2
5	3	A <sub>1</sub>	A <sub>2</sub>	8355.772	8355.747	.025	3
5	1	E <sub>2</sub>	A <sub>2</sub>	8367.932	8367.941	-.009	2
5	2	E <sub>2</sub>	A <sub>2</sub>	8368.849	8368.863	-.014	2
5	4	E <sub>2</sub>	A <sub>2</sub>	8363.976	8363.970	.006	4
5	5	E <sub>2</sub>	A <sub>2</sub>	8361.866	8361.861	.005	2
5	1	A <sub>1</sub>	E	8357.080	8357.043	.037	2
5	2	A <sub>1</sub>	E	8356.549	8356.585	-.036	2
5	4	A <sub>1</sub>	E	8354.386	8354.409	-.023	3
5	0	E <sub>2</sub>	E	8368.443	8368.396	.047	2
5	2	E <sub>2</sub>	E	8365.158	8365.190	-.032	4
5	3	E <sub>2</sub>	E	8367.799	8367.854	-.055	5
5	4	E <sub>2</sub>	E	8365.710	8365.703	.007	4
6	1	E <sub>2</sub>	A <sub>1</sub>	8411.732	8411.742	-.010	2
6	1	E <sub>2</sub>	A <sub>2</sub>	8408.707	8408.678	.029	2
7	1	E <sub>2</sub>	A <sub>1</sub>	8458.945	8458.945	.000	3

<sup>a</sup> N is the number of assigned transitions of the energy levels.

into account while we fitted the (310; E<sub>1</sub>) band independently. The least-squares fit was performed with a model in which the A<sub>1</sub> and E vibrational states were treated simultaneously because of the strong vibrational-rotational interactions.

The diagonal matrix elements for the A state take the customary form

$$H_s = \langle v; Jk | H | v; Jk \rangle = G_s + B_s[J(J+1) - k^2] + C_s k^2 - D_s^J J^2(J+1)^2 - D_{JK}^s J(J+1)k^2 - D_K^s k^4 + \dots \quad [1]$$

The corresponding expression for the E state takes the form

$$H_t = \langle vl; Jk | H | vl; Jk \rangle = G_t + B_t[J(J+1) - k^2] + C_t k^2 - 2(C\zeta)_t kl - D_t^J J^2(J+1)^2 - D_{JK}^t J(J+1)k^2 - D_K^t k^4 + \eta_{JJ}^t J(J+1)kl + \eta_K^t k^3 + \eta_{JK}^t J(J+1)k^3 l + \eta_{kk}^t k^5 l \dots \quad [2]$$

For the off-diagonal parameters, we consider the resonance of the H<sub>22</sub> term given below,

$$\langle 310E^+; Jk + 2 | H | 310E^-; Jk \rangle = \frac{1}{2} \{ q_{\text{eff}} + q_{\text{eff}}^J J(J+1) \} F(J, k) F(J, k+1), \quad [3]$$

$$\langle 310E^-; Jk + 1 | H | 310E^+; Jk \rangle = 2r_{\text{eff}}(2k+1)F(J, k), \quad [4]$$

and

$$\langle 310E^+; Jk + 1 | H | 310A_1; Jk \rangle = \langle 310A_1; Jk + 1 | H | 310E^-; Jk \rangle = \frac{1}{2\sqrt{2}} \{ \alpha_{\text{eff}}^{\text{zx}}(2k+1) + \alpha_{\text{eff}}^{\text{zx}'} J(J+1)(2k+1) + \alpha_{\text{eff}}^{\text{zx}''} [k^3 + (k+1)^3] \} F(J, k), \quad [5]$$

where  $F(J, k) = \sqrt{J(J+1) - k(k+1)}$ .

All the other off-diagonal resonance terms cannot be fitted well and are excluded from the present study.

## 5. THE VIBRATIONAL ANALYSIS

The stretching potential surface of AsH<sub>3</sub> has been optimized in Ref. (3) using a local mode model, the anharmonically coupled anharmonic oscillators (ACAO) model. In this earlier work, only eight stretching band centers, most of which are from medium-resolution work, were used as input

TABLE 3  
Energy Levels ( $\text{cm}^{-1}$ ) of the 310;  $E_1$  State of  $\text{AsH}_3$

J	K	Sym. of Vib.	Sym.	Obs.	Cal.	Obs.-Cal.	N <sup>a</sup>
0	0	E <sub>1</sub>	E	8257.273	8257.273	.000	1
1	1	E <sub>1</sub>	A <sub>2</sub>	8264.646	8264.586	.060	1
1	0	E <sub>1</sub>	E	8264.452	8264.439	.013	1
1	1	E <sub>1</sub>	E	8263.747	8263.744	.003	1
2	1	E <sub>1</sub>	A <sub>1</sub>	8278.793	8278.888	-.095	1
2	2	E <sub>1</sub>	A <sub>1</sub>	8277.076	8277.083	-.007	2
2	1	E <sub>1</sub>	A <sub>2</sub>	8279.021	8279.043	-.022	1
2	2	E <sub>1</sub>	A <sub>2</sub>	8277.076	8277.083	-.007	2
2	0	E <sub>1</sub>	E	8278.796	8278.781	.015	1
2	1	E <sub>1</sub>	E	8278.074	8278.057	.017	1
2	2	E <sub>1</sub>	E	8278.390	8278.372	.018	1
3	1	E <sub>1</sub>	A <sub>1</sub>	8300.614	8300.632	-.018	1
3	2	E <sub>1</sub>	A <sub>1</sub>	8298.447	8298.458	-.011	1
3	1	E <sub>1</sub>	A <sub>2</sub>	8300.402	8300.355	.047	1
3	2	E <sub>1</sub>	A <sub>2</sub>	8298.447	8298.458	-.011	1
3	0	E <sub>1</sub>	E	8300.314	8300.319	-.005	1
3	1	E <sub>1</sub>	E	8299.519	8299.534	-.015	1
3	2	E <sub>1</sub>	E	8299.922	8299.953	-.031	1
3	3	E <sub>1</sub>	E	8297.270	8297.261	.009	2
4	1	E <sub>1</sub>	A <sub>1</sub>	8328.998	8329.004	-.006	1
4	2	E <sub>1</sub>	A <sub>1</sub>	8326.966	8326.966	.000	2
4	4	E <sub>1</sub>	A <sub>1</sub>	8325.772	8325.771	.001	2
4	2	E <sub>1</sub>	A <sub>2</sub>	8326.966	8326.966	.000	2
4	4	E <sub>1</sub>	A <sub>2</sub>	8325.772	8325.771	.001	2
4	0	E <sub>1</sub>	E	8329.094	8329.073	.021	1
4	2	E <sub>1</sub>	E	8328.693	8328.692	.001	3
4	3	E <sub>1</sub>	E	8325.480	8325.464	.016	2
4	3	E <sub>1</sub>	E	8327.689	8327.680	.009	2
4	4	E <sub>1</sub>	E	8323.779	8323.780	-.001	2
5	1	E <sub>1</sub>	A <sub>1</sub>	8365.296	8365.296	.000	4
5	2	E <sub>1</sub>	A <sub>1</sub>	8362.512	8362.518	-.006	1
5	4	E <sub>1</sub>	A <sub>1</sub>	8362.937	8362.942	-.005	2
5	5	E <sub>1</sub>	A <sub>1</sub>	8355.454	8355.457	-.003	3
5	2	E <sub>1</sub>	A <sub>2</sub>	8362.512	8362.518	-.006	1
5	4	E <sub>1</sub>	A <sub>2</sub>	8362.937	8362.942	-.005	2
5	5	E <sub>1</sub>	A <sub>2</sub>	8355.454	8355.457	-.003	3
5	0	E <sub>1</sub>	E	8364.613	8364.597	.016	4
5	1	E <sub>1</sub>	E	8363.811	8363.818	-.007	2
5	2	E <sub>1</sub>	E	8365.041	8365.034	.007	2
5	3	E <sub>1</sub>	E	8360.696	8360.695	.001	1
5	3	E <sub>1</sub>	E	8364.245	8364.249	-.004	1
5	4	E <sub>1</sub>	E	8358.350	8358.343	.007	3
5	5	E <sub>1</sub>	E	8361.120	8361.116	.004	2

<sup>a</sup> N is the number of assigned transitions of the energy levels.

data. Recently we have carried out a series of high-resolution spectroscopic studies of  $\text{AsH}_3$  stretching bands from  $\nu = 2$  up to 6. We found that the observed local mode combination band centers are always smaller than the calculations in Ref. (3). For example, the observed (310;A<sub>1</sub>) band center is smaller than the calculated values (see Table 5 of Ref. (3))

by  $3.6 \text{ cm}^{-1}$ . The reason for this discrepancy is that the least-squares fitting of Ref. (3) uses only two local mode combination bands with a 10 times larger uncertainty than the fundamentals. Hence it is worthwhile to repeat this fitting by including the new high-resolution data. As can be seen below, the fitting results agree better with the observation

TABLE 4  
Observed and Calculated Stretching Band Centers of AsH<sub>3</sub> (in cm<sup>-1</sup>)<sup>a</sup>

$\nu$	States	obs.	Cal.		Ref.
			Model 1	Model 2	
1	100A <sub>1</sub>	2115.16	2114.50	2114.08	13
	E	2126.42	2125.71	2125.57	13
2	200A <sub>1</sub>	4166.77	4165.82	4165.34	7
	E	4167.94	4167.21	4166.97	7
	110A <sub>1</sub>	4237.70	4237.54	4237.16	this work
	E	4247.53	4247.49	4247.41	this work
3	300A <sub>1</sub>	6136.34	6136.01	6135.72	8
	E	6136.33	6136.08	6135.83	8
	210A <sub>1</sub>	6275.83	6275.78	6275.95	this work
	E <sub>1</sub>	6282.36	6282.18	6282.54	this work
	E <sub>2</sub>	6294.71	6295.13	6294.81	this work
	A <sub>2</sub>		6299.70	6299.63	
	111A <sub>1</sub>	6365.96	6366.20	6366.36	this work
	400A <sub>1</sub>	8028.97	8028.80	8028.73	9
4	E	8028.97	8028.80	8028.74	9
	310A <sub>1</sub>	8249.52	8250.60	8250.95	this work
	E <sub>1</sub>		8252.47	8252.97	
	E <sub>2</sub>	8258.38	8259.03	8259.68	this work
	A <sub>2</sub>		8260.78	8261.54	
	220A <sub>1</sub>		8333.47	8333.63	
	E		8334.82	8335.20	
	211A <sub>1</sub>		8395.78	8397.04	
5	E		8417.04	8417.44	
	500A <sub>1</sub> /E	9841.40 <sup>b</sup>	9845.08	9845.34	this work
6	600A <sub>1</sub> /E	11576.30 <sup>b</sup>	11584.90	11585.64	10
7	700A <sub>1</sub> /E		13248.28	13249.63	
8	800A <sub>1</sub> /E		14835.20	14837.32	
9	900A <sub>1</sub> /E		16345.67	16348.72	

<sup>a</sup> All the observed data are given equal weights in the fitting except for the 500 and 600 bands.

<sup>b</sup> Not included in the fitting due to perturbations.

of the local mode combination bands. For example, the 3.6 cm<sup>-1</sup> difference mentioned above has been reduced to 1.1 and 1.3 cm<sup>-1</sup> for potential models I and II, respectively.

The ACAO model used in the fitting has been detailed in Ref. (3). Briefly, the AsH<sub>3</sub> molecule is considered as a set of three Morse oscillators coupled to one another by kinetic and potential coupling terms in the ACAO model. Only three

parameters are required: the two parameters  $D_e$  and  $a$  of the Morse oscillators and the parameter of the potential coupling, which is assumed to be of the form  $f_{rr'rr'}$  (potential model I) or of the form  $f_{rr'yy'}$  with  $y$  being the Morse variable  $y = 1 - \exp(-ar)$  (potential model II). In practical calculation, the maximum total vibrational quantum number is set to 12, and the valence angle is set to its equilibrium

TABLE 5  
Stretching Potential Energy Parameters for Arsine<sup>a</sup>

Parameters	ACAO I	ACAO II
$a$ (°)	1.501156(987)	1.500129(1464)
$D_e$ (cm <sup>-1</sup> )	31643.7(364)	31669.1(542)
$f_{rr'}$ (cm <sup>-1</sup> Å <sup>2</sup> )	-412.1(134)	-455.1(222)
$s$ (cm <sup>-1</sup> )	0.59	0.87

<sup>a</sup> Uncertainties in parentheses are one standard error in the last figure quoted.  $s$  is the standard deviation of the fit.

value  $q_e = 92.069^\circ$ . The observed and calculated stretching band centers are given in Table 4, and the optimized stretching potential parameters are given in Table 5. The standard deviation of the fit is 0.59 and 0.87 cm<sup>-1</sup> for potential model I and model II, respectively. The fitting result confirms our previous vibrational assignment of the (310;  $A_1$ ) and (310;  $E_2$ ) bands, while the weaker  $E$  symmetry band observed at 8257.27 cm<sup>-1</sup> cannot be convincingly assigned to the (310;  $E_1$ ) band which, according to the calculation, is located 4.3 cm<sup>-1</sup> higher. We noticed that the stretch-bend combination band ( $210 + 2\nu_4^{\pm 2}$ ) is quite close to the (310) band, and perturbation due to this band could cause the shift of the (310;  $E_1$ ) band from its predicted position.

## 6. DISCUSSION

Our analysis of the (210) band systems found good agreement between the calculated and observed effective  $H_{22}$ -type constants. However, the current analysis found significant discrepancies between the calculated and observed values in

the (310) band systems. Hence the predictions of  $H_{22}$ -type constants are not listed. These discrepancies are probably due to the rotational perturbations not considered in the present fitting. Particularly the perturbation due to the ( $210 + 2\nu_4^{\pm 2}$ ) band is considered important.

## ACKNOWLEDGMENTS

This work was supported by the Chinese Academy of Sciences and, in part, by the Russian Foundation on Fundamental Research. Oleg N. Ulenikov thanks the University of Science and Technology of China in Hefei for the professorship during April–May 1996.

## REFERENCES

1. S. L. Coy and K. K. Lehmann, *J. Chem. Phys.* **84**, 5239–5249 (1986); K. K. Lehmann and S. L. Coy, *J. Chem. Soc. Faraday Trans. 2* **84**, 1389–1406 (1988); S. L. Coy and K. K. Lehmann, *Spectrochim. Acta* **45**, 47–56 (1989).
2. G. Tarrago, N. Lacombe, A. Levy, G. Guelachvili, B. Bézard, and P. Drosstart, *J. Mol. Spectrosc.* **154**, 30–42 (1992).
3. M. Halonen, L. Halonen, H. Bürger, and P. Moritz, *J. Phys. Chem.* **96**, 4225–4231 (1992).
4. M. Halonen, L. Halonen, H. Bürger, and P. Moritz, *J. Chem. Phys.* **95**, 7099–7107 (1991).
5. M. Halonen, L. Halonen, H. Bürger, and P. Moritz, *Chem. Phys. Lett.* **203**, 157–163 (1993).
6. J. Lummila, T. Lukka, L. Halonen, H. Bürger, and O. Polanz, *J. Chem. Phys.* **104**, 488–498 (1996).
7. S. F. Yang, X. G. Wang, and Q. S. Zhu, *Spectrochim. Acta, Part A* **53**, 157–163 (1997).
8. O. N. Ulenikov, F. G. Sun, X. G. Wang, and Q. S. Zhu, *J. Chem. Phys.* **105**, 7310–7315 (1996).
9. J. X. Cheng, X. G. Wang, H. Lin, and Q. S. Zhu, *Chin. Phys. Lett.* **14**, 656–659 (1997).
10. J. X. Han, O. N. Ulenikov, S. Yurchinko, L. Y. Hao, X. G. Wang, and Q. S. Zhu, *Spectrochim. Acta, Part A* **53**, 1705–1712 (1997).
11. R. A. Toth, *Appl. Opt.* **33**, 4851–4867 (1994).
12. M. Carlotti, G. D. Lonardo, and L. Fusina, *J. Mol. Spectrosc.* **102**, 310–319 (1983).
13. O. N. Ulenikov, A. E. Cheglovkov, and G. A. Shevchenko, *J. Mol. Spectrosc.* **157**, 141–160 (1993).